Am J Transl Res 2022;14(9):6550-6562
www.ajtr.org /ISSN:1943-8141/AJTR0144093

Original Article

The integrative network of circRNA, miRNA and mRNA of epicardial adipose tissue in patients with atrial fibrillation

Hong Zheng[1*], Yuanshu Peng[2*], Pan Wang[3], Pixiong Su[2], Lei Zhao[3]

[1]Comprehensive Ward of Cardiology, Beijing An Zhen Hospital, Capital Medical University, Beijing 100029, China; [2]Department of Cardiac Surgery, Heart Center and Beijing Key Laboratory of Hypertension, Beijing Chaoyang Hospital, Capital Medical University, Beijing 100020, China; [3]Heart Center and Beijing Key Laboratory of Hypertension, Beijing Chaoyang Hospital, Capital Medical University, Beijing 100020, China. [*]Equal contributors.

Received May 12, 2022; Accepted August 4, 2022; Epub September 15, 2022; Published September 30, 2022

Abstract: Introduction: Atrial fibrillation (AF) is a highly prevalent cardiac arrhythmia that affects approximately 1-2% of the general population. The mechanism of AF pathogenesis remains unclear. Epicardial adipose tissue (EAT), a metabolically active visceral fat depot surrounding the heart, has been shown to be closely related to AF. EAT has a biological impact on neighboring myocardium by producing a myriad of bioactive molecules, including exosomes carrying circular RNAs (circRNAs). As a new category of noncoding RNAs, circRNAs can work as efficient sponges for specific microRNAs and efficiently regulate gene expression. Material and Methods: To investigate the regulatory mechanism of circRNAs of EAT in patients with AF, we collected EAT from AF (n=6) patients and non-AF (n=6) controls and profiled their circRNA expression with the RNA-sequencing method. Results: RNA sequencing detected a total of 2159 circRNAs in EAT, among which 528 were upregulated and 579 were downregulated. The top highly expressed EAT circRNAs corresponded to genes involved in inflammation and cell proliferation, including SUPT5H, CCDC62, DPY19L1P1, RASGRP1, AP3S1, CGNL1, KAT2B, BNIP2, and SACS. The top three circRNAs with higher FCs (fold changes) were hsa_circ_0099634, hsa_circ_0000932 and hsa_circ_0097669 (FC=25.6), while lower FCs were identified in hsa_circ_0135289, hsa_circ_0098155 and hsa_circ_0079672. A network involving these noncoding RNAs and mRNAs was also constructed to predict their potential biological functions in the pathology of AF. Conclusions: Our study provided novel insight into EAT's roles in AF and proposed interactions, including possible mediators.

Keywords: Atrial fibrillation, epicardial adipose tissue, noncoding RNA, circular RNA, microRNA

Introduction

Atrial fibrillation (AF), as the most common cardiac arrhythmia, is a growing epidemic and a major cause of ischemic stroke and heart failure, which are the leading causes of morbidity and mortality worldwide [1-3]. Multiple mechanisms underlying AF include atrial electrophysiological and structural remodeling, characterized by increased myocardial fibrosis and heterogeneous conduction abnormalities, which ultimately promote AF perpetuation and the progression to permanent AF [4]. Some risk factors are related to AF pathophysiology, but the potential molecular indicators involved in this process still need to be clarified. Despite remarkable progress in the prevention and treatment of AF, its pathogenesis remains largely unknown. Thus, gaining insight into the pathogenesis of AF and searching for new treatments are of utmost importance.

Epicardial adipose tissue (EAT), a metabolically active visceral fat located in atrioventricular and interventricular grooves, has been shown to function as a metabolic transducer in the regulation of cardiac functions [5-7]. Several clinical observational studies with cardiac imaging techniques have identified a close association between EAT and AF [8-10]. The EAT volume quantified by computed tomography and thickness measured by echocardiography also predicted AF catheter ablation outcome independent of left atrial size and body mass index

(BMI) [11-13]. EAT has a biological impact on neighboring myocardium by producing a myriad of bioactive molecules, including exosomes carrying noncoding RNAs (ncRNAs). The main groups of ncRNAs include microRNAs (miRNAs), long noncoding RNAs, and circular RNAs (circRNAs). CircRNAs are an ever-growing class of ncRNAs with a covalently closed loop structure [14, 15]. Due to the lack of a typical terminal 5' cap and 3' polyadenylated tail, they are presumably less prone to enzymolysis by exonucleases. With the development of high-throughput technologies, abundant and diverse circRNAs have been identified and annotated [16, 17]. As reported, these circRNAs can act as efficient sponges targeting specific miRNAs and efficiently regulate gene expression [15, 18]. In addition to their roles as novel biomarkers in diagnosis, circRNAs are also considered important epigenetic modulators participating in various pathophysiological processes, and their important functions in cardiac conditions are becoming increasingly apparent [15, 19-21]. These circRNAs can be sorted into exosomes along with other nucleic acids and lipids and released into the extracellular environment, where they can reach recipient cells and elicit functional responses [22]. However, their role in EAT, especially in the process of AF, has not been precisely defined.

Therefore, in this study, we aimed to identify the regulatory mechanism of circRNAs in EAT associated with AF and clarify the interactions among circRNAs and miRNAs and their mRNA targets. Our study provided novel insights into the role of EAT in AF and constructed a highly possible network involving circRNAs, miRNAs and mRNAs.

Materials and methods

Study participants and sample collection

We collected EAT from six persistent nonvalvular AF patients and six sinus rhythm patients undergoing coronary artery bypass grafting. Persistent AF was defined as a sustained episode lasting > 7 days. The exclusion criteria were the presence of pregnancy, serum potassium > 5 mmol/L, New York Heart Association (NYHA) grading > II, left atrial appendage thrombosis, neoplasm, severe liver or renal disease, or other infectious or inflammatory conditions. Epicardial biopsy samples (volume 1-2 cm^3) were obtained before the initiation of cardiopulmonary bypass and were taken along the atrioventricular groove or from the anterior surface of the heart near the anterior descending coronary artery. After collection, the samples were cut into small pieces, washed with PBS, quickly frozen in liquid nitrogen and finally stored at -80°C until analysis. This study was approved by the Ethical Committee of Beijing Chaoyang Hospital (2021-ke-246) and performed in compliance with the guidelines of the 1975 Declaration of Helsinki. All the enrolled patients provided written informed consent.

RNA sequencing analysis

RNA was extracted from EAT using miRNAeasy Mini Kits (Qiagen) according to the manufacturer's instructions, and concentrations were checked by a Nanodrop 1000 spectrophotometer. All RNA samples displayed a 260/280-absorbance ratio ≤ 2.0. A total of 1-2 μg of RNA was used to construct a sequencing library. First, ribosomal RNA (rRNA) was removed using the RiboZero Magnetic Gold Kit. Then, sequencing libraries were generated using a KAPA Stranded RNA-Seq Library Prep Kit for Illumina. The DNA fragments were amplified in situ using a TruSeq SR Cluster Kit v3-cBot-HS (#GD-401-3001, Illumina) and then sequenced by running 150 cycles. The resulting libraries were qualified on the Agilent Bioanalyzer 2100 system and subsequently sequenced on the Illumina HiSeq 4000 platform. After base quality was filtered by FastQC (http://www.bioinformatics.babraham.ac.uk/projects/fastqc/), the raw sequencing reads were subjected to adapter trimming (5', 3'-adaptor bases were trimmed and ≤ 20 bp reads were filtered using Cutadapt software). High-quality reads were mapped to the human reference genome using HISAT 2 software, and the fragments per kilobase of gene/transcript model per million mapped fragments (FPKM) values of known genes and transcripts were measured using Ballgown in the R package via the transcript abundances estimated with StringTie. Fold change (FC) > 1.5, a P value < 0.05 and FPKM ≥ 0.05 were set for the filtration of differentially expressed transcripts.

Identification of the differentially expressed circRNAs

The quantification of the backsplice junction read count in circRNA was aligned to the transcriptome using STAR software to detect junction sites and then calculated with CIRCexplorer 2. The mean values of counts per million reads (CPM) in each group ≥ 100 were consid-

Table 1. Demographic and clinical characteristics of patients

Characteristics	Non-AF (n=6)	AF (n=6)	*P* value
Age, years	63 ± 7	59 ± 9	0.319
Male, n, %	4 (66.7%)	3 (50%)	1.0
BMI, kg/m^2	25.1 ± 5.3	24.8 ± 4.7	0.693
Systolic blood pressure, mmHg	114 ± 19	135 ± 16	0.066
Diastolic blood pressure, mmHg	69 ± 8	77 ± 5	0.085
Diabetes, n, %	2 (33.3%)	0	0.455
Hypertension, n, %	4 (66.7%)	3 (50%)	1.0
Leukocytes, ×10^9/L	7.7 ± 2.1	8.6 ± 1.7	0.436
Hemoglobin, g/L	131 ± 10	140 ± 26	0.428
BNP, ng/L	387.7 ± 321.2	193.8 ± 161.9	0.254
ESR, mm/h	8.6 ± 11.6	19.0 ± 9.0	0.151
C-reactive protein, mg/L	3.5 ± 5.0	10.6 ± 0.8	0.05
Fast glucose, mmol/L	5.5 ± 0.5	7.2 ± 3.5	0.255
Total cholesterol, mmol/L	4.3 ± 0.8	4.7 ± 2.1	0.657
LDL, mmol/L	2.8 ± 0.7	3.3 ± 1.9	0.563
HDL, mmol/L	1.2 ± 0.3	0.9 ± 0.2	0.094
Triglycerides, mmol/L	1.3 ± 0.4	1.2 ± 0.2	0.562
Uric acid, μmol/L	354.9 ± 80.7	381.8 ± 65.6	0.541
BUN, mmol/L	6.0 ± 2.6	6.8 ± 2.9	0.62
Serum creatinine, μmol/L	68.6 ± 9.5	75.1 ± 17.2	0.436
LVEDD, mm	51 ± 9	51 ± 7	1.0
LVEF, %	57.3 ± 5.0	62.8 ± 7.5	0.17

AF, atrial fibrillation; BMI, body mass index; BNP, brain natriuretic peptide; BUN, blood urea nitrogen; ESR, erythrocyte sedimentation rate; HDL, high density lipoprotein; HF, heart failure; LDL, low density lipoprotein; LVEDD, left ventricular end diastolic diameter; LVEF, left ventricular ejection fraction.

ered to be significantly expressed and analyzed statistically. The statistical significance of differential expression between AF and non-AF groups was calculated with a t test in the R software package and further filtered by fold change. CircRNAs with a *P* value < 0.05 and FC greater than 1.5 were considered to be significant. Hierarchical clustering analysis arranged samples into groups based on FPKM values, and the resulting dendrogram showed the relationships among expression patterns. Scatter plots and volcano plots were also generated with log2-scaled FPKM.

Construction of the integrative regulatory network of circRNAs, miRNAs and mRNAs

CircRNAs can work as endogenous sponges for miRNAs by competing with miRNA/mRNA binding or as decoys for RNA-binding proteins to potentially modulate gene expression. Then, we constructed integrative network models with circRNAs, miRNAs and target mRNAs to explore the relationship between noncoding RNAs and mRNAs of EAT in the pathogenesis of AF. The interaction network was built using homemade miRNA target prediction software based on TargetScan and miRanda [23, 24] and visually presented via Cytoscape software based on the screening of circRNA-miRNA pairs. Since no special annotation information was available for circRNAs, we carried Gene Ontology (GO) enrichment analysis (http://www.geneontology.org) and Kyoto Encyclopedia of Genes and Genomes (KEGG) pathway analysis (http://www.genome.jp/kegg) to investigate the possible biological functions.

Statistics

In the clinical dataset, categorical variables are expressed as frequencies and percentages, and continuous variables are expressed as means ± standard deviations. Comparisons between groups were performed using independent-sample t tests for continuous variables and the chi-square or Fisher's exact tests for categorical variables. These analyses were performed with IBM SPSS Statistics 24.0, and a 2-tailed *P* value < 0.05 was considered significant. Hierarchical clustering and network construction were performed in R, Python or the shell environment for statistical computing, and detailed statistics for each analysis are described in the corresponding sections.

Results

Differentially expressed circRNAs in EAT associated with atrial fibrillation

This study investigated the changes in the transcriptomes of epicardial adipose samples in AF patients (n=6) and non-AF subjects (n=6) by RNA sequencing. The baseline demographic and clinical parameters are presented in **Table 1**. RNA sequencing produced paired-end reads

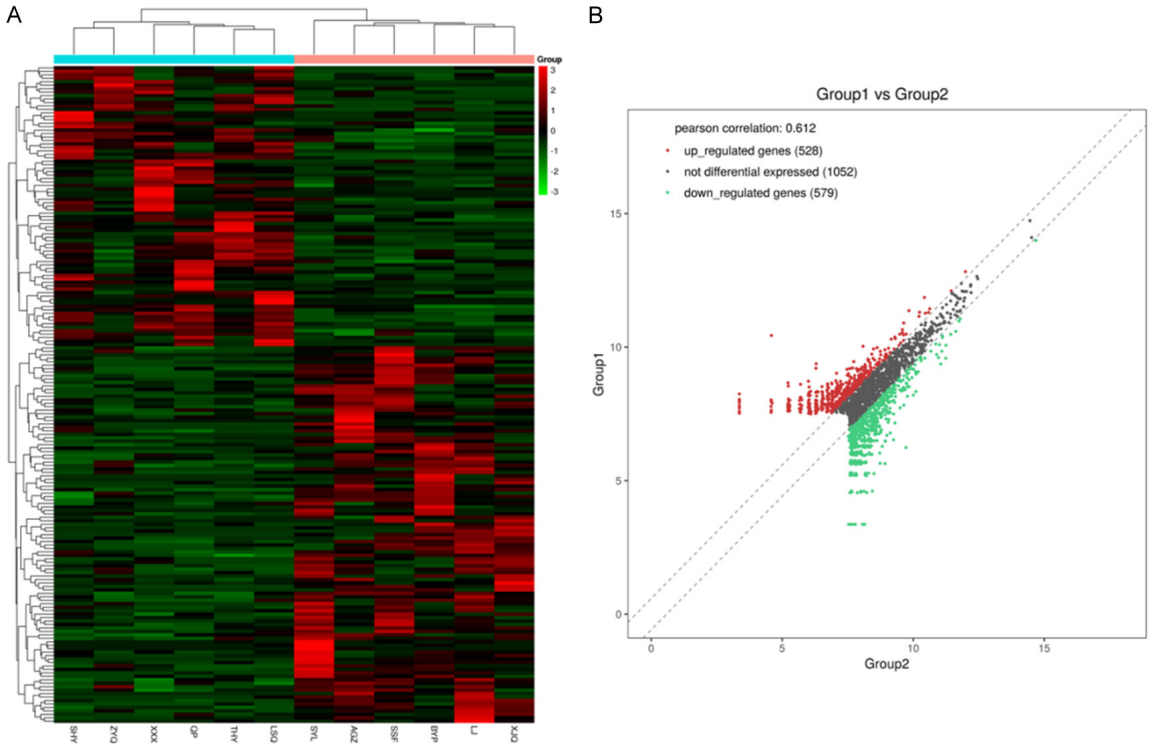

Figure 1. The hierarchical clustering (A) and scatter plot (B) of the differentially expressed circRNAs in patients with or without atrial fibrillation. A total of 2159 circRNA were identified, of which 528 were up-regulated and 579 down-regulated.

with sufficient quality and read coverage per sample to perform further analysis. The Pearson R2 correlation analysis suggested high correlation among individual samples of each group, and principal component analysis revealed a distinguishable gene expression profile between the two groups (Supplementary Figure 1).

RNA sequencing detected a total of 2159 circRNAs in EAT, and the length of the detected circRNAs ranged mainly within 2000 nt (Supplementary Table 1). Hierarchical clustering analysis was performed to arrange samples into groups based on FPKM values, allowing us to hypothesize the relationships between groups. The hierarchical clustering heatmap and scatter plot are depicted in **Figure 1**. Among 2159 circRNAs identified with P < 0.05, 528 were upregulated and 579 were downregulated. Ten circRNAs were exclusively detected in EAT with AF. Among these exclusively expressed circRNAs, nine were already functionally described and recorded in circBase: hsa_circ_0000932 (SUPT5H generated), hsa_circ_0097669 (CCDC62 generated), hsa_circ_0006010 (DPY19L1P1 generated), hsa_circ_0034414 (RASGRP1 generated), hsa_circ_0002919 (AP3S1 generated), hsa_circ_0035436 (CGNL1 generated), hsa_circ_0123308 (KAT2B generated), hsa_circ_0035537 (BNIP2 generated), and hsa_circ_0002046 (SACS generated) (Supplementary Table 2).

Differentially expressed circRNAs were recognized if the t test *P* value < 0.05 and the FC was greater than 1.5. Accordingly, there were 81 upregulated circRNAs and 109 downregulated circRNAs in EAT with AF patients. These differentially expressed circRNAs are detailed in Supplementary Table 3 and visualized as a volcano plot in **Figure 2**. The top three circRNAs with higher FCs were hsa_circ_0099634 (FC=57.6), hsa_circ_0000932 (FC=29.5) and hsa_circ_0097669 (FC=25.6), while lower FCs were identified in hsa_circ_0135289 (FC=0.036), hsa_circ_0098155 (FC=0.039), and hsa_circ_0079672 (FC=0.046). Then, these six candidate circRNAs were verified by quanti-

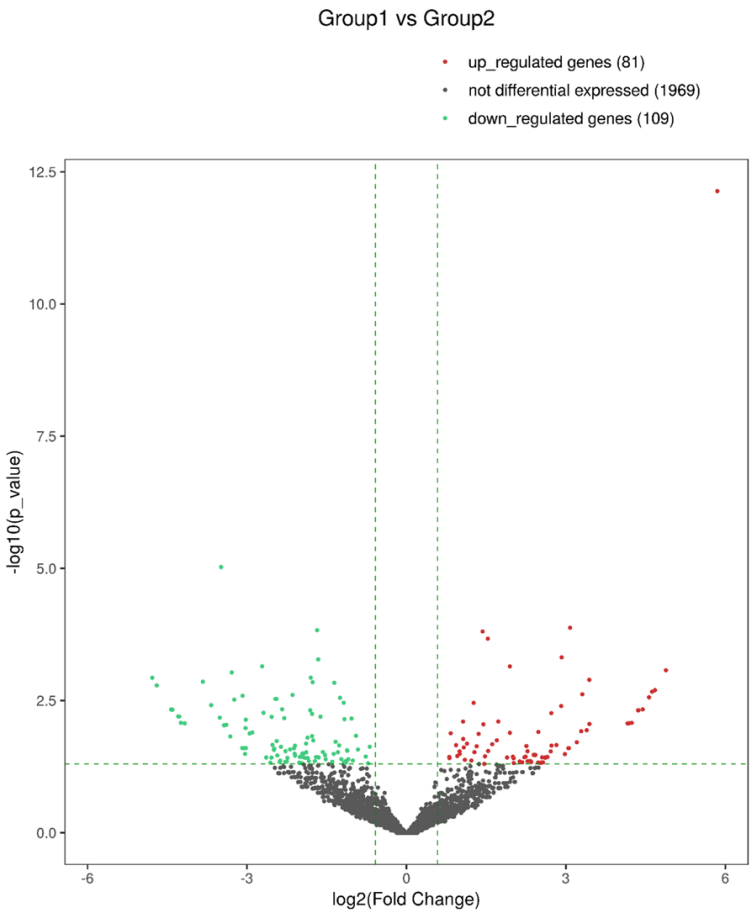

Figure 2. The volcano plot of the differentially expressed circRNAs of epicardial adipose tissue in atrial fibrillation and controls ($P < 0.05$; fold change > 1.5).

tative real-time polymerase chain reaction (**Figure 3**).

CircRNA-miRNA interactions in atrial fibrillation

Based on the interactions between ncRNAs and mRNAs, a competing endogenous RNA (ceRNA) circRNA-miRNA-mRNA network (**Figure 3**) was constructed to predict their potential biological functions in the pathology of AF. This network provided preliminary insight into the links between these six circRNAs and their target miRNA and genes, which finally showing a large interaction network (**Figure 4**).

We performed GO enrich analysis, including biological processes, cell components and molecular function analysis (**Figure 5**). Most target genes focused on cellular nitrogen compound biosynthetic process, SCF-dependent proteasomal ubiquitin-dependent protein catabolic process and macromolecule biosynthetic process. Based on the KEGG database, the top ten enriched score of significant pathways were analyzed and shown in **Figure 6**. These target genes may play a role in lipid and atherosclerosis, herpes simplex virus 1 infection and PI3K-AKT signaling pathway.

We limited target miRNAs less than 2000, and built circRNA-miRNA-mRNA network again (**Figure 7**). This network involved two circRNAs (hsa_circRNA_000932 and hsa_circ_0078619), 48 miRNAs, and nine mRNAs targeting the following genes: KANK4, TRIM55, MCOLN1, PSMD12, CD68, ISM1, HOXA2, EIF5B and TRDN (Supplementary Table 4), which suggested that a regulatory cross-talk network relied on the sponging capacity of circRNAs. hsa_circ_0078619 interacted with both upregulated and downregulated miRNAs, while hsa_circ_0000932 interacted with only three miRNAs, miR-7704, miR-663a and miR-6787-5p, one of which, miR-663a, contributed to LPS-induced NF-κB activation and the autoimmune inflammatory response [25] and was involved in the modulation of collagen 4 secretion under physiological conditions and in response to ER stress [26].

Discussion

As a novel category of endogenous ncRNAs, circRNAs have been recently reported to function as efficient miRNA sponges to compete with pre-mRNA splicing and serve as circRNA-protein interactions. Recent studies have suggested that circRNAs may contribute to the development of cardiovascular diseases, suggesting that circRNAs can work as novel therapeutic targets [27, 28]. As reported, Foxo3-derived circRNA induced senescence in fib-

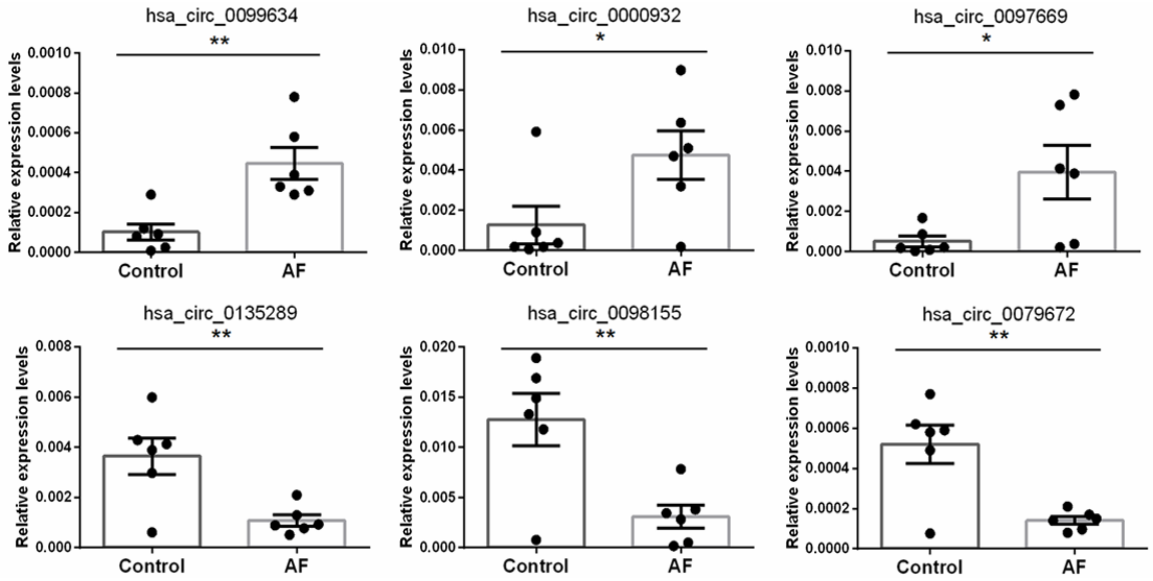

Figure 3. QT-PCR verification of six candidate circRNAs. The data are normalized using the mean ± SEM (*P < 0.05; **P < 0.01; n=6 per group).

roblasts in vitro through binding to and sequestering proteins involved in the cellular stress response, such as hypoxia-inducible factor 1α and focal adhesion kinase [18, 29]. Additionally, overexpression of circNFIB can attenuate cardiac fibrosis by sponging miR433 [30], and targeting the highly abundant circSlc8a1 in cardiomyocytes, which functions as endogenous sponge for miR133a, and probably alleviates pressure overload-induced hypertrophy [31]. Additionally, circAmotl1 was shown to potentiate AKT-enhanced cardiomyocyte survival and enhance cardiac repair in vivo [32]. CircRNAs are mainly expressed in a tissue- and development stage-specific pattern, and a subset is conserved across species. In addition to their endogenous actions, circRNAs can be secreted into the extracellular space within nanoparticles termed exosomes [22, 33, 34]. These cell-derived exosomes contain numerous circRNAs, which can function locally or enter the circulation to relocate to distal cells. Currently, circRNAs have been reported to be concentrated in serum exosomes, leading us to hypothesize that epicardial adipose cells secrete exosomal circRNAs to regulate atrial electrical and structural remodeling, which underlie the biological interactions between EAT and its neighboring myocardium in AF [22].

In the present study, we provided a comprehensive circRNA profile of human EAT associated with AF. A total of 2159 circRNAs were identified, including ten circRNAs of EAT exclusively expressed in AF. Interestingly, all of these exclusively expressed circRNAs were upregulated in our analysis. Following the collection of differentially expressed mRNAs and circRNAs in our sequencing analysis, we wove a circRNA-miRNA-mRNA interactional network. In the first analysis, we constructed a large interaction network including six circRNAs and their various miRNA and target genes. Then, we rebuilt a limited network and found that hsa_circRNA_000932 and hsa_circ_0078619 may work as endogenous RNAs to capture various miRNAs, such as miR-103a-2-5p and miR-199a-5p, and subsequently regulate the expression of KANK4, TRIM55, MCOLN1, PSMD12, CD68, ISM1, HOXA2, EIF5B and TRDN. Many of these protein-coding genes have been reported to be part of the regulation in cardiovascular disorders. For instance, since TRDN encodes Triadin, which is associated with the release of calcium ions, the loss of which contributes to impaired excitation-contraction coupling and cardiac arrhythmias [35], and even the common variants in TRDN are closely related to an increased risk of sudden cardiac death in chronic heart failure [36]. Additionally, the expression of tripartite motif-containing 55 (TRIM55) was found to be reduced in patients with idiopathic dilated cardiomyopathy [37]. Among these microRNAs (micRNAs), some have been identified to be associated with car-

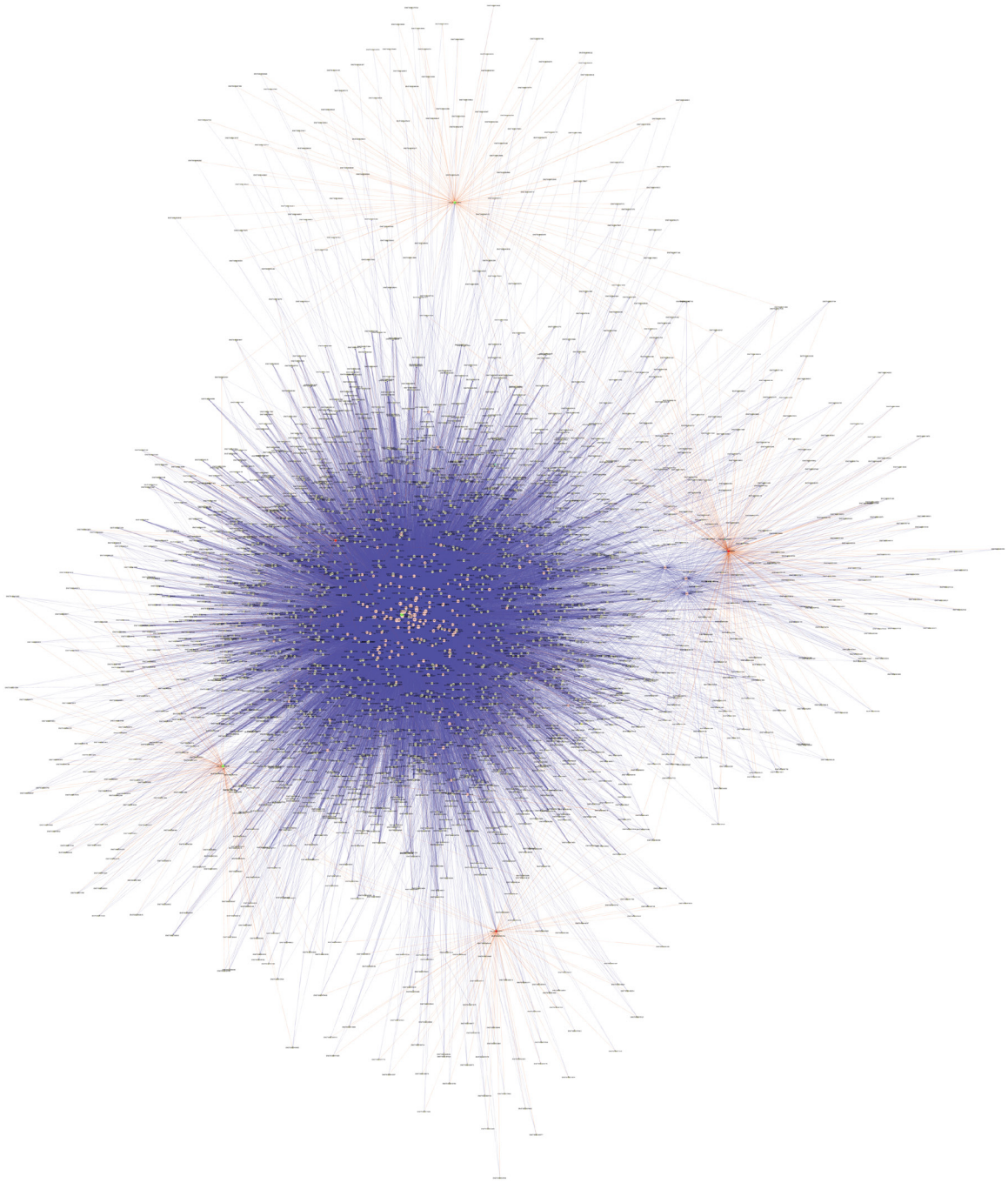

Figure 4. An integrative regulatory network model of six circRNAs and their target miRNAs and mRNAs of epicardial adipose tissue in atrial fibrillation.

diac remodeling. hsa-miR-103a-2-5p has been reported to modulate oxidative stress in hypertension via the regulation of poly-(ADP-ribose) polymerase [38]. In addition, hsa-miR-1283 has been shown to regulate the PERK/ATF4 pathway, which plays a critical role in inducing injury in HUVECs and mouse heart tissue [39]. Additionally, the levels of circulating hsa-miR-106a-5p were associated with increasing acuity of heart failure [40]. Of note, miR-199a-5p was identified to be upregulated in paroxysmal AF [41] and targeted FKBP5 or FK506-binding protein 5, which may inhibit store-operated calcium entry through the I_{soc} channel [42].

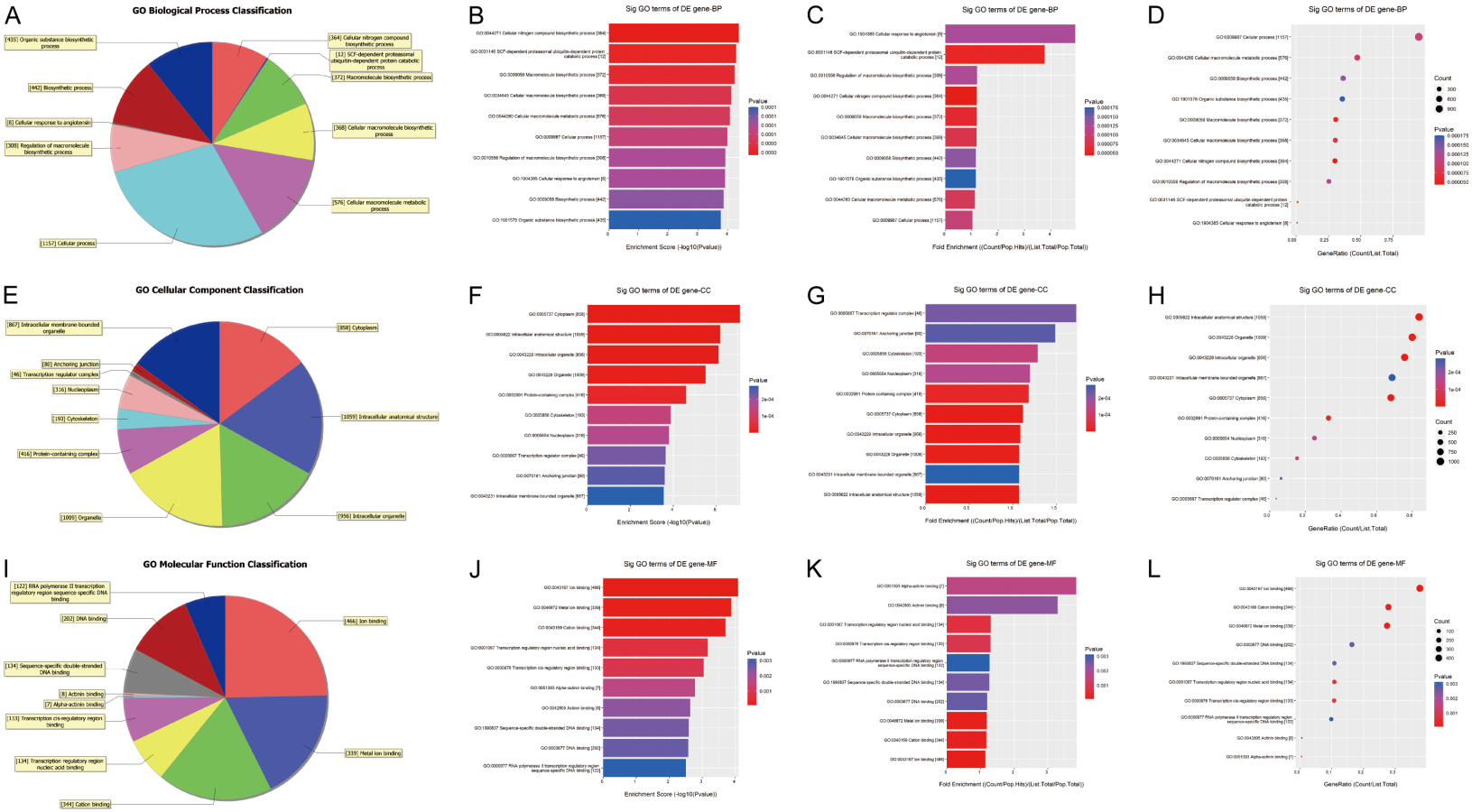

Figure 5. The GO annotations for biological process (A-D), cellular components (E-H) and molecular function (I-L) of target mRNAs regulated by the six candidate circRNAs.

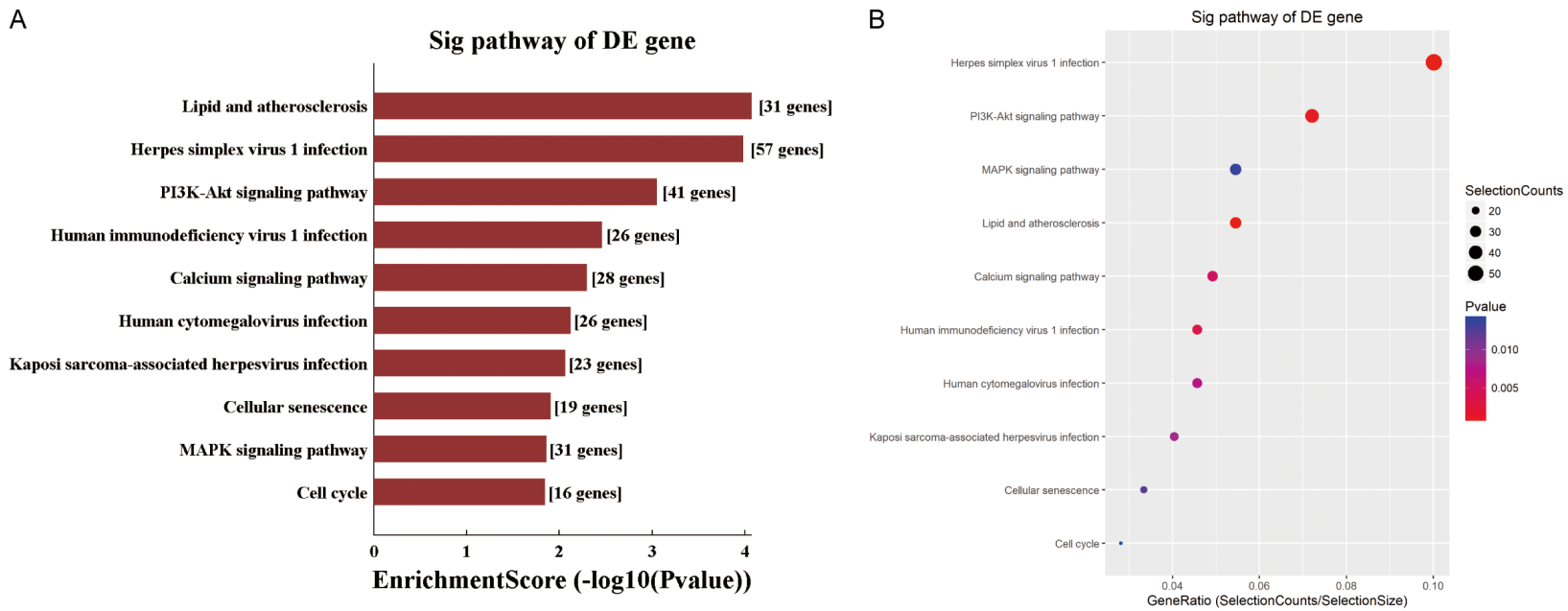

Figure 6. KEGG pathway analysis of target genes regulated by the six circRNAs. The bar plot (A) and dot plot (B) showed the top ten enrichment score values of the significantly enriched pathway.

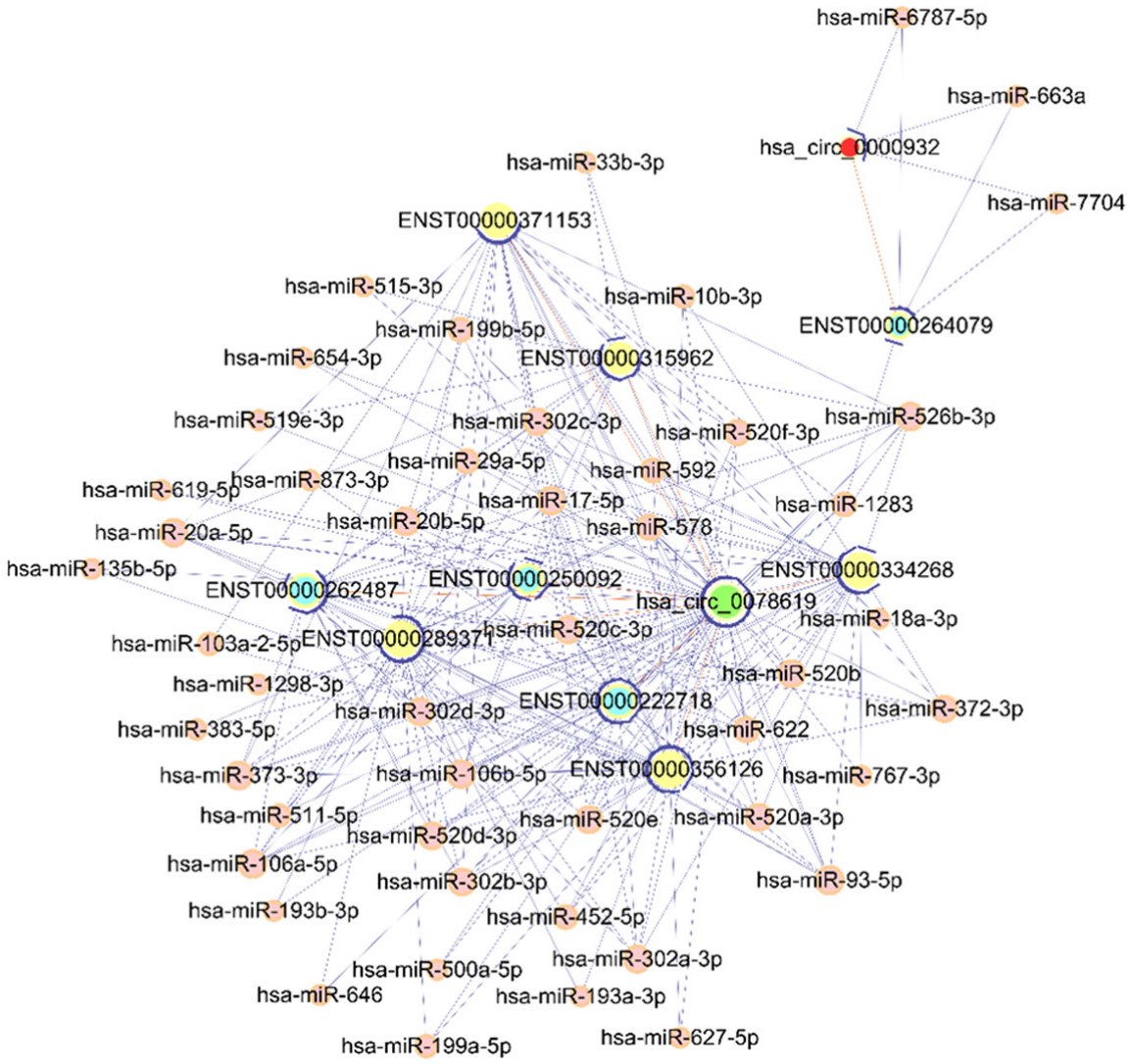

Figure 7. The limited circRNA-miRNA-mRNA network consisting of two circRNAs (hsa_circRNA_000932 and hsa_circ_0078619), 48 miRNAs, and nine genes was generated by Cytoscape. Nodes with pink color represent miRNAs. Nodes with light-green and red colors represent down- and up-circRNAs, respectively, while nodes with light-blue and yellow colors represent up- and down-coding RNAs. Edges with T-shape arrow represent directed relationships, while the rest represent undirected relationships.

Given that the trigger and progression of AF are both complex pathological processes, the biological role of EAT in AF involving circRNAs should be studied. Although we identified differentially expressed circRNAs in EAT via RNA sequencing, further investigations are needed to characterize the crosstalk mechanism between circRNAs and target miRNAs. Subgroup analysis of circRNAs should also be performed to explore the regulatory function. Since our analyses were mainly based on an in silico approach, proper experimental models are needed to decipher the role of ncRNAs in AF.

In summary, for the first time, we explored and analyzed the expression patterns of circRNAs in epicardial adipose samples with AF. These data present a comprehensive profile of circRNAs in EAT involved in the development of AF and construct a ceRNA network among circRNAs, miRNAs and mRNAs, providing a novel insight into potential pathways that may be involved in the pathogenesis of AF. Thus, targeting the circRNA-miRNA-mRNA ceRNA network in EAT has emerged as a prewarning biomarker and a novel therapeutic approach against the progression of AF. More investigations will be

required to define the physiological functions and underlying mechanisms by which these circRNAs and the ceRNA network in EAT modulate the structural and functional remodeling of the atrium in the progression of AF.

Disclosure of conflict of interest

None.

Address correspondence to: Lei Zhao and Pixiong Su, Heart Center and Beijing Key Laboratory of Hypertension, Beijing Chaoyang Hospital, Capital Medical University, Beijing 100020, China. Tel: +86-10-85231939; Fax: +86-10-85231939; E-mail: lily885300@sina.com (LZ); supixiong1130@163.com (PXS)

References

[1] Zimetbaum P. Atrial fibrillation. Ann Intern Med 2017; 166: C33-C48.

[2] Poudel P, Xu Y, Cui Z, Sharma D, Tian B and Paudel S. Atrial fibrillation: recent advances in understanding the role of microRNAs in atrial remodeling with an electrophysiological overview. Cardiology 2015; 131: 58-67.

[3] Zhao L, Wang W and Yang X. Anticoagulation in atrial fibrillation with heart failure. Heart Fail Rev 2018; 23: 563-571.

[4] Wong CX, Ganesan AN and Selvanayagam JB. Epicardial fat and atrial fibrillation: current evidence, potential mechanisms, clinical implications, and future directions. Eur Heart J 2017; 38: 1294-1302.

[5] Hatem SN, Redheuil A and Gandjbakhch E. Cardiac adipose tissue and atrial fibrillation: the perils of adiposity. Cardiovasc Res 2016; 109: 502-509.

[6] Hatem SN and Sanders P. Epicardial adipose tissue and atrial fibrillation. Cardiovasc Res 2014; 102: 205-213.

[7] Zhao L, Harrop DL, Ng A and Wang W. Epicardial adipose tissue is associated with left atrial dysfunction in people without obstructive coronary artery disease or atrial fibrillation. Can J Cardiol 2018; 34: 1019-1025.

[8] Vroomen M, Olsthoorn JR, Maesen B, L'Espoir V, La Meir M, Das M, Maessen JG, Crijns H, Verheule S and Pison L. Quantification of epicardial adipose tissue in patients undergoing hybrid ablation for atrial fibrillation. Eur J Cardiothorac Surg 2019; 56: 79-86.

[9] Klein C, Brunereau J, Lacroix D, Ninni S, Brigadeau F, Klug D, Longere B, Montaigne D, Pontana F and Coisne A. Left atrial epicardial adipose tissue radiodensity is associated with electrophysiological properties of atrial myocardium in patients with atrial fibrillation. Eur Radiol 2019; 29: 3027-3035.

[10] Bos D, Vernooij MW, Shahzad R, Kavousi M, Hofman A, van Walsum T, Deckers JW, Ikram MA, Heeringa J, Franco OH, van der Lugt A and Leening MJG. Epicardial fat volume and the risk of atrial fibrillation in the general population free of cardiovascular disease. JACC Cardiovasc Imaging 2017; 10: 1405-1407.

[11] Thanassoulis G, Massaro JM, O'Donnell CJ, Hoffmann U, Levy D, Ellinor PT, Wang TJ, Schnabel RB, Vasan RS, Fox CS and Benjamin EJ. Pericardial fat is associated with prevalent atrial fibrillation: the Framingham Heart Study. Circ Arrhythm Electrophysiol 2010; 3: 345-350.

[12] Kocyigit D, Gurses KM, Yalcin MU, Turk G, Evranos B, Yorgun H, Sahiner ML, Kaya EB, Hazirolan T, Tokgozoglu L, Oto MA, Ozer N and Aytemir K. Periatrial epicardial adipose tissue thickness is an independent predictor of atrial fibrillation recurrence after cryoballoon-based pulmonary vein isolation. J Cardiovasc Comput Tomogr 2015; 9: 295-302.

[13] Yorgun H, Canpolat U, Aytemir K, Hazirolan T, Sahiner L, Kaya EB, Kabakci G, Tokgozoglu L, Ozer N and Oto A. Association of epicardial and peri-atrial adiposity with the presence and severity of non-valvular atrial fibrillation. Int J Cardiovasc Imaging 2015; 31: 649-657.

[14] Zaiou M. Circular RNAs in hypertension: challenges and clinical promise. Hypertens Res 2019; 42: 1653-1663.

[15] Aufiero S, Reckman YJ, Pinto YM and Creemers EE. Circular RNAs open a new chapter in cardiovascular biology. Nat Rev Cardiol 2019; 16: 503-514.

[16] Tan WL, Lim BT, Anene-Nzelu CG, Ackers-Johnson M, Dashi A, See K, Tiang Z, Lee DP, Chua WW, Luu TD, Li PY, Richards AM and Foo RS. A landscape of circular RNA expression in the human heart. Cardiovasc Res 2017; 113: 298-309.

[17] Werfel S, Nothjunge S, Schwarzmayr T, Strom TM, Meitinger T and Engelhardt S. Characterization of circular RNAs in human, mouse and rat hearts. J Mol Cell Cardiol 2016; 98: 103-107.

[18] Devaux Y, Creemers EE, Boon RA, Werfel S, Thum T, Engelhardt S, Dimmeler S and Squire I. Circular RNAs in heart failure. Eur J Heart Fail 2017; 19: 701-709.

[19] Li JJ, Wang W, Wang XQ, He Y, Wang SS and Yan YX. A novel strategy of identifying circRNA biomarkers in cardiovascular disease by meta-analysis. J Cell Physiol 2019; 234: 21601-21612.

[20] Li M, Duan L, Li Y and Liu B. Long noncoding RNA/circular noncoding RNA-miRNA-mRNA

axes in cardiovascular diseases. Life Sci 2019; 233: 116440.
[21] Sallam T, Sandhu J and Tontonoz P. Long noncoding RNA discovery in cardiovascular disease: decoding form to function. Circ Res 2018; 122: 155-166.
[22] Wang Y, Liu J, Ma J, Sun T, Zhou Q, Wang W, Wang G, Wu P, Wang H, Jiang L, Yuan W, Sun Z and Ming L. Exosomal circRNAs: biogenesis, effect and application in human diseases. Mol Cancer 2019; 18: 116.
[23] Garcia DM, Baek D, Shin C, Bell GW, Grimson A and Bartel DP. Weak seed-pairing stability and high target-site abundance decrease the proficiency of lsy-6 and other microRNAs. Nat Struct Mol Biol 2011; 18: 1139-1146.
[24] Grimson A, Farh KK, Johnston WK, Garrett-Engele P, Lim LP and Bartel DP. MicroRNA targeting specificity in mammals: determinants beyond seed pairing. Mol Cell 2007; 27: 91-105.
[25] Wang W, Gao J and Wang F. MiR-663a/MiR-423-5p are involved in the pathogenesis of lupus nephritis via modulating the activation of NF-kappaB by targeting TNIP2. Am J Transl Res 2017; 9: 3796-3803.
[26] Amodio G, Sasso E, D'Ambrosio C, Scaloni A, Moltedo O, Franceschelli S, Zambrano N and Remondelli P. Identification of a microRNA (miR-663a) induced by ER stress and its target gene PLOD3 by a combined microRNome and proteome approach. Cell Biol Toxicol 2016; 32: 285-303.
[27] Gao X, Tian X, Huang Y, Fang R, Wang G, Li D, Zhang J, Li T and Yuan R. Role of circular RNA in myocardial ischemia and ageing-related diseases. Cytokine Growth Factor Rev 2022; 65: 1-11.
[28] Huang S, Li X, Zheng H, Si X, Li B, Wei G, Li C, Chen Y, Chen Y, Liao W, Liao Y and Bin J. Loss of super-enhancer-regulated circRNA Nfix induces cardiac regeneration after myocardial infarction in adult mice. Circulation 2019; 139: 2857-2876.
[29] Du WW, Yang W, Chen Y, Wu ZK, Foster FS, Yang Z, Li X and Yang BB. Foxo3 circular RNA promotes cardiac senescence by modulating multiple factors associated with stress and senescence responses. Eur Heart J 2017; 38: 1402-1412.
[30] Zhu Y, Pan W, Yang T, Meng X, Jiang Z, Tao L and Wang L. Upregulation of circular RNA CircNFIB attenuates cardiac fibrosis by sponging miR-433. Front Genet 2019; 10: 564.
[31] Lim TB, Aliwarga E, Luu T, Li YP, Ng SL, Annadoray L, Sian S, Ackers-Johnson MA and Foo RS. Targeting the highly abundant circular RNA circSlc8a1 in cardiomyocytes attenuates pressure overload induced hypertrophy. Cardiovasc Res 2019; 115: 1998-2007.
[32] Zeng Y, Du WW, Wu Y, Yang Z, Awan FM, Li X, Yang W, Zhang C, Yang Q, Yee A, Chen Y, Yang F, Sun H, Huang R, Yee AJ, Li RK, Wu Z, Backx PH and Yang BB. A circular RNA binds to and activates AKT phosphorylation and nuclear localization reducing apoptosis and enhancing cardiac repair. Theranostics 2017; 7: 3842-3855.
[33] Shah RV, Rong J, Larson MG, Yeri A, Ziegler O, Tanriverdi K, Murthy V, Liu X, Xiao C, Pico AR, Huan T, Levy D, Lewis GD, Rosenzweig A, Vasan RS, Das S and Freedman JE. Associations of circulating extracellular RNAs with myocardial remodeling and heart failure. JAMA Cardiol 2018; 3: 871-876.
[34] Cai B, Ma W, Ding F, Zhang L, Huang Q, Wang X, Hua B, Xu J, Li J, Bi C, Guo S, Yang F, Han Z, Li Y, Yan G, Yu Y, Bao Z, Yu M, Li F, Tian Y, Pan Z and Yang B. The long noncoding RNA CAREL controls cardiac regeneration. J Am Coll Cardiol 2018; 72: 534-550.
[35] Chopra N, Yang T, Asghari P, Moore ED, Huke S, Akin B, Cattolica RA, Perez CF, Hlaing T, Knollmann-Ritschel BE, Jones LR, Pessah IN, Allen PD, Franzini-Armstrong C and Knollmann BC. Ablation of triadin causes loss of cardiac Ca2+ release units, impaired excitation-contraction coupling, and cardiac arrhythmias. Proc Natl Acad Sci U S A 2009; 106: 7636-7641.
[36] Liu Z, Liu X, Yu H, Pei J, Zhang Y, Gong J and Pu J. Common variants in TRDN and CALM1 are associated with risk of sudden cardiac death in chronic heart failure patients in chinese han population. PLoS One 2015; 10: e132459.
[37] Prestes PR, Marques FZ, Lopez-Campos G, Booth SA, Mcglynn M, Lewandowski P, Delbridge LM, Harrap SB and Charchar FJ. Tripartite motif-containing 55 identified as functional candidate for spontaneous cardiac hypertrophy in the rat locus cardiac mass 22. J Hypertens 2016; 34: 950-958.
[38] Dluzen DF, Kim Y, Bastian P, Zhang Y, Lehrmann E, Becker KG, Noren HN and Evans MK. MicroRNAs modulate oxidative stress in hypertension through PARP-1 regulation. Oxid Med Cell Longev 2017; 2017: 3984280.
[39] He L, Yuan J, Xu Q, Chen R, Chen L and Fang M. MiRNA-1283 regulates the PERK/ATF4 pathway in vascular injury by targeting ATF4. PLoS One 2016; 11: e159171.
[40] Ovchinnikova ES, Schmitter D, Vegter EL, Ter Maaten JM, Valente MA, Liu LC, van der Harst P, Pinto YM, de Boer RA, Meyer S, Teerlink JR, O'Connor CM, Metra M, Davison BA, Bloomfield DM, Cotter G, Cleland JG, Mebazaa A, Laribi S, Givertz MM, Ponikowski P, van der Meer P, van Veldhuisen DJ, Voors AA and Berezikov E. Signature of circulating microRNAs in patients with acute heart failure. Eur J Heart Fail 2016; 18: 414-423.

[41] Chiang DY, Zhang M, Voigt N, Alsina KM, Jakob H, Martin JF, Dobrev D, Wehrens XH and Li N. Identification of microRNA-mRNA dysregulations in paroxysmal atrial fibrillation. Int J Cardiol 2015; 184: 190-197.

[42] Dong F, Skinner DC, Wu TJ and Ren J. The heart: a novel gonadotrophin-releasing hormone target. J Neuroendocrinol 2011; 23: 456-463.

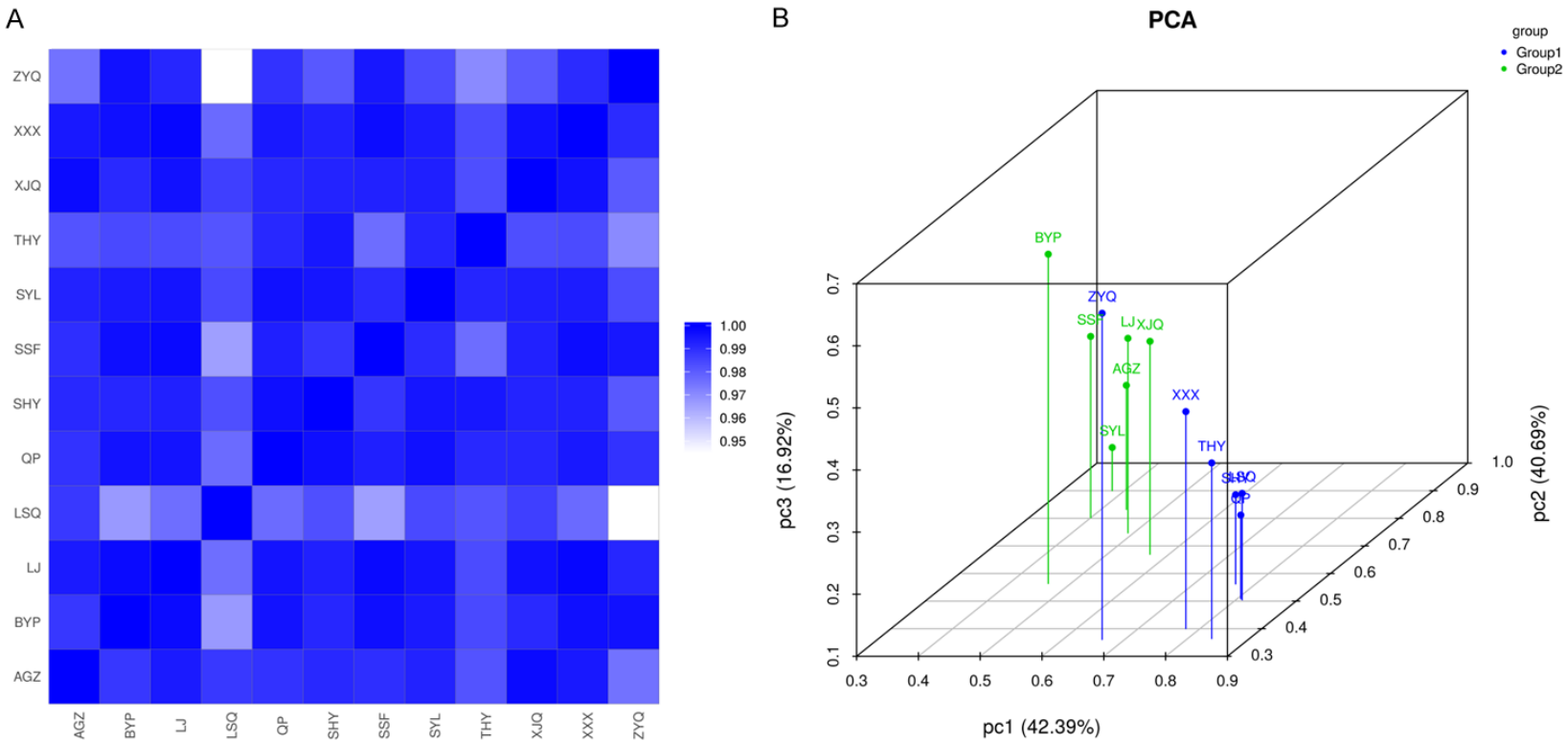

Supplementary Figure 1. Correlation analysis and principal component analysis. A. Heatmap of Pearson correlation. Blue color indicates high correlation and white color indicates low correlation. B. Principal component analysis (PCA) plot for all EAT samples. PCA was performed with genes that show the ANOVA *P* value < 0.05 on FPKM abundance estimation.